

# Dewetting as an investigative tool for studying properties of thin polymer films

G. Reiter<sup>1,a,b</sup>, S. Al Akhrass<sup>1</sup>, M. Hamieh<sup>1</sup>, P. Damman<sup>2</sup>, S. Gabriele<sup>2,3</sup>, T. Vilmin<sup>4</sup>, and E. Raphaël<sup>4</sup>

<sup>1</sup> Institut de Chimie des Surfaces et Interfaces, UHA-CNRS, 68057 Mulhouse Cedex, France

<sup>2</sup> Laboratoire de Physicochimie des Polymères, Centre d'Innovation et de Recherche en Matériaux Polymères (CIRMAP), Université de Mons Hainaut, 20 place du Parc, 7000 Mons, Belgium

<sup>3</sup> Materia Nova Asbl, Parc Initialis, 1 avenue N. Copernic, 7000 Mons, Belgium

<sup>4</sup> Laboratoire de Physico-Chimie Théorique, UMR CNRS Gulliver 7083, ESPCI, 10 rue Vauquelin, 75231 Paris Cedex 05, France

**Abstract.** Employing mass conservation, time-resolved dewetting experiments of thin polymer films allow to determine in real time the dynamic contact angle and the slippage length. Moreover, based on a systematic variation of interfacial properties of a polymer brush, dewetting makes it possible to calculate the force it needs to extract a single polymer chain from its own melt. In the visco-elastic regime close to the glass transition, the temperature and molecular weight dependence of the relaxation time of residual stresses resulting from film preparation by spin-coating can be obtained from the evolution of the shape of the dewetting rim. The presented examples demonstrate that dewetting represents a powerful approach for a sensitive characterization of rheological, frictional and interfacial properties of thin polymer films.

## 1 Introduction

The phenomenon of dewetting, that is the retraction of a fluid from a surface it was forced to cover, is frequently observed in our everyday life and is of central importance in many technological applications as well as in a variety of physical and biological systems [1]. The wettability of a surface by a liquid is to a large extent characterized by the interfacial tensions and is reflected by the contact angle. However, it is difficult to investigate kinetic effects like friction (energy dissipation) at an interface by contact angle measurements alone. The necessary velocity-dependent information is provided by spreading or dewetting experiments [2–24]. In this context, thin polymer films provide convenient systems due to their high viscosity (enabling time resolved measurements) and their non-volatility (assuring mass conservation).

Dewetting experiments are attractive because of their simplicity, sensitivity and rapidity. Dewetting allows to link molecular and interfacial properties (and variations thereof) with macroscopically observable parameters like dewetting velocity and shape of the rim. Despite its simplicity with respect to experimental observation it turns out that dewetting is extremely sensitive to even tiniest changes in the studied system. Dewetting has proven to be a highly successful and time-efficient tool for obtaining time-resolved information on a molecular scale, allowing to determine interfacial properties and their changes in real time and in situ [9–24].

<sup>a</sup> e-mail: guenter.reiter@physik.uni-freiburg.de

<sup>b</sup> Present address: Physikalisches Institut, Universität Freiburg, Hermann-Herder-Str. 3, 79104 Freiburg, Germany

Besides measuring the temporal evolution of the dewetted distance, additional quantitative information can be obtained simultaneously from a detailed analysis of the shape of the rim and its evolution. Theoretical understanding, very much advanced by the work of Françoise Brochard [2,4–8], helped to set-up appropriate experiments.

In general, the displacement of a contact line reflects kinetic effects at a polymer-polymer interface. Due to the balance of (capillary) driving forces and energy dissipation at the interface as a consequence of intrinsic properties controlled by molecular interactions, a dewetting film is at all stages self-adjusting to any variations of experimental conditions. The main driving force for dewetting is due to an imbalance between the three interfacial tensions of the liquid-air, liquid-substrate, and substrate-air interfaces which meet at the three-phase contact line. This capillary force (uncompensated Young force) is related to the difference between the dynamic (during dewetting) and the equilibrium contact angle. In the course of dewetting of supported films, the removed liquid is generally collected in a rim just ahead of the moving contact line, where most of the invested energy is dissipated. In this presentation, we would like to demonstrate via a few examples that this balance of forces enables us to extract highly quantitative and detailed information on molecular and interfacial properties of thin polymer films from relatively simple dewetting experiments.

## 2 Experimental section

We present experimental results on the dewetting behaviour of thin polymer films on smooth non-wettable silicon substrates. In the first part, we have used thin polydimethylsiloxane (PDMS) films supported by silicon wafers which were coated with a layer of end-grafted PDMS molecules [9,10,25,26]. At high grafting densities an autophobic behaviour was observed [9,10], i.e., the free molecules dewetted the grafted layer. In the second part, we replaced the PDMS films by polystyrene (PS) films of different molecular weights ( $M_w$  was 52, 125 and 5000 kDa, respectively, with a polydispersity index lower than 1.10). The thickness of the films was measured by ellipsometry and was in the range of 30 to 150 nm. All films were obtained by spin-coating rather dilute solutions (heptane for PDMS and toluene for PS) directly onto the coated substrates. Dewetting of PS films was induced by heating of the sample on a nitrogen-purged hot stage above the glass transition temperature. Isothermal dewetting of the thin polymer films, i.e. the retraction of a contact line, was followed in real time ( $t$ ) by optical microscopy (AFM). Images were captured with a CCD camera. The morphology of the rim was also investigated with an Atomic Force Microscope. More details on sample preparation and dewetting measurements can be found in [9,10].

As has been shown previously, polystyrene thin films spin-coated onto PDMS-coated silicon wafers are unstable and typically dewet via the formation of holes. In addition, a PS film can also retract from the edge of the sample [12,13,15,23,24]. Dewetting of PS was followed for times shorter than the longest relaxation time of polymer chains in bulk, i.e. the reptation time. During these stages, viscoelasticity dominated the dewetting behaviour.

## 3 Results and discussion

During dewetting of a Newtonian fluid, the driving capillary force  $F_d$  is balanced by viscous forces  $F_v$  (forces per unit length of the three-phase contact line) [2–10]. In a good approximation,  $F_d$  is determined by the contact angle ( $\theta$ ) and the surface tension ( $\gamma$ ) of the liquid as  $F_d = 0.5\gamma\theta^2$ .  $F_v$  depends on the hydrodynamics of liquid flow. For non-slipping films exhibiting Poiseuille flow (see Fig. 1(a)), the main part of the invested capillary energy is dissipated in a small volume located near the contact line. Then,  $F_v$  is simply proportional to the viscosity ( $\eta$ ) and the velocity ( $V$ ). In such dewetting experiments,  $V$  remains constant in time. However, long polymers on a non-adsorbing substrate have been found to slip [27]. There, the main part of the capillary energy is dissipated over the whole moving part of the film proportional to the

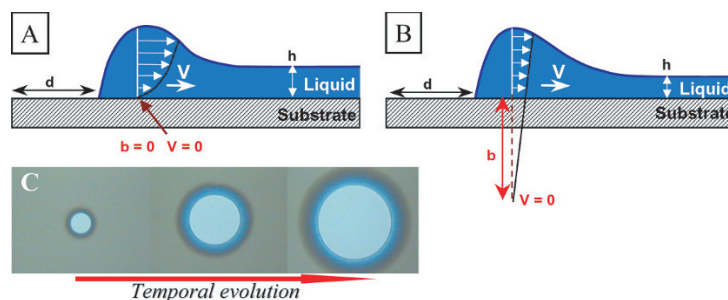


**Fig. 1.** Schematic presentation of dewetting at A) a non-slipping and B) a slipping substrate. C) Characteristic temporal evolution of dewetting (hole growth) for a 50 nm thick polystyrene film ( $M_w = 52$  kg/mol) at  $120^\circ\text{C}$  for 5, 30 and 60 min, respectively. The size of each of the three images is  $59 \times 47 \mu\text{m}^2$ .

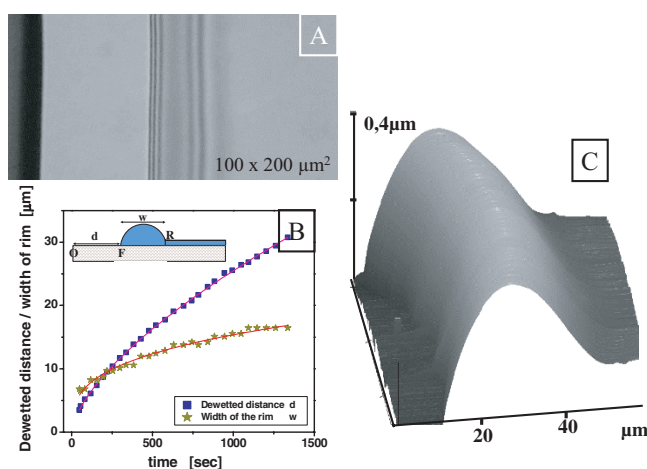


**Fig. 2.** Typical result for dewetting of a PDMS film (92 nm,  $M_w = 308$  kg/mol) on top of a densely grafted brush of end-functionalised PDMS molecules (6.3 nm,  $M_w = 8.8$  kg/mol). The temperature was  $50^\circ\text{C}$ . A) Optical micrograph (top view) of dewetting. B) Temporal evolution of dewetted distance  $d$  and the width  $w$  of the rim, schematically represented in the inset. The lines are best fits of  $y = A(t - t_o)^\alpha$  to the data where  $y$  stands for  $d$  and  $w$ ,  $A$  is a constant pre-factor, and  $t_o$  is the time offset.  $\alpha$  was found to be 0.65 and 0.32 for  $d$  and  $w$ , respectively. For details see [9,10]. C) 3D-view of the shape of the rim as measured by atomic force microscopy.

width ( $w$ ) of the rim formed by the liquid from the dewetted region of a film of thickness ( $h$ ) [5–10]. In this case (see Fig. 1(b)),

$$F_v = 3h \cdot V \cdot w/b \quad (1)$$

with  $b$  being the slippage length that characterizes the degree of “slippiness”.

Independent of the boundary condition, the growth of a dewetting hole always follows a path similar to the one shown in Fig. 1(c) for a slipping polystyrene hole on a PDMS-coated substrate. An example for a more systematic analysis of a dewetting experiment is given in Fig. 2 for autophobic dewetting of a PDMS film. Here, we want to point out the possibility of simultaneously measuring the dewetted distance ( $d$ ) and the width ( $w$ ) of the rim by tracking the front ( $F$ ) and rear ( $R$ ) positions of the dewetting rim in time. In Fig. 2(b), both  $d$  and  $w$  did not increase linearly in time, i.e. the dewetting velocity decreased in the course of dewetting. Fitting the data points for  $d$  in Fig. 2(b) to a power-law gave an exponent of 0.65 for  $d(t)$  which is consistent with the theoretically expected [5,6] value of  $2/3$  for slippage of the liquid on the substrate.

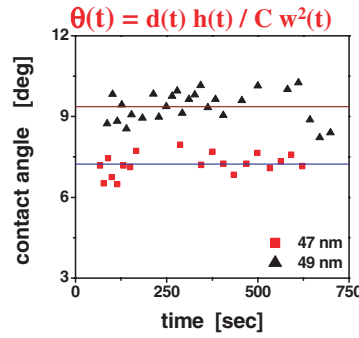


**Fig. 3.** Examples for the temporal evolution of the contact angle in the course of dewetting as derived from mass conservation for the system described in Fig. 2 (thicknesses are indicated in the figure).

Based on mass conservation, measuring  $d$  and  $w$  for nonvolatile liquids like polymers as a function of time  $t$  allows to determine and even to track the value of  $\theta$  in time, without any fitting. For slipping films we get:

$$\theta(t) = d(t) \cdot h(t) / Cw^2(t). \quad (2)$$

The constant  $C$ , accounting for the shape of the rim, has been found [5] to be 0.1 for slipping films. Typical results of autophobic dewetting of PDMS films are shown in Fig. 3. The values of  $\theta$  differed between samples but were found to be constant in time, confirming the stability and homogeneity of the investigated dewetting system.

According to eq. (1), the viscous force  $F_v$  increases with  $w$ . Taking into account the balance of forces ( $F_d = F_v$ ) and knowing that in the course of the dewetting experiments described in Fig. 2 the driving force characterized by  $\theta$  is constant (see Fig. 3), we anticipate that the dewetting velocity  $V$  decreases with the increase in  $w$ . This is indeed confirmed in Fig. 4(a) by presenting the dewetting velocity  $V(t_i)$ , derived by taking differences,  $V(t_i) = [d(t_i) - d(t_{i-1})] / (t_i - t_{i-1})$  as a function of  $w$ . For samples of different thickness (but identical contact angle) the results superposed on a single curve.

Based on the concept of a continuous balance of forces and using eq. (1), dewetting experiments also allow to determine  $b$  and possible variations in  $b$  in the course of an experiment [9], reflecting changes in the molecular structure of the liquid/substrate interface, for any time interval  $t_i - t_{i-1}$ , without making any assumptions about the temporal evolution of  $d$  and  $w$  (see Fig. 4(b)). Interestingly, these results indicate that for the slow dewetting velocities of these experiments,  $b$  did not depend on dewetting velocity nor on film thickness.

The slippage length  $b$  can also be presented [27] as the ratio of viscosity  $\eta$  over the interfacial friction coefficient  $\zeta$  (per area of a monomer,  $a^2$ ):  $b = \eta / \zeta$ . Thus, for the observed values of  $b \approx 10 \mu\text{m}$  and the viscosity of the dewetting PDMS film ( $\eta = 1000 \text{ Pa} \cdot \text{s}$ ) we can deduce a value of  $\zeta \approx 10^8 \text{ Pa} \cdot \text{s}/\text{m}$ . Comparing this value to the monomeric friction coefficient [28]  $\zeta_o = 3.7 \times 10^7 \text{ Pa} \cdot \text{s}/\text{m}$  indicates that only a few monomers at the interface contributed to friction ( $\zeta \approx 3\zeta_o$ ), thereby implying that the free polymers penetrated only little into the layer of densely grafted, chemically identical polymers. In conclusion, this example shows that dewetting experiments are capable of relating friction at the brush-melt interface to the degree of interpenetration between grafted and free polymer chains.

Raphaël and de Gennes [29] predicted that in order to pull out a polymer chain from its own melt, a certain threshold force  $F_p$  has to be overcome. Accordingly, when dewetting a substrate coated with a bimodal brush as shown in Fig. 5(a), the long chain “connectors” resist to be pull out. Consequently, the driving capillary forces ( $F_d$ ) are diminished by the resisting pull-out force ( $F_p$ ) due to the connectors and the resulting dewetting velocity is derived from the balance with viscous forces ( $F_v$ ) (all forces are per unit length of the contact line):

$$F_d - F_p = F_v. \quad (3)$$

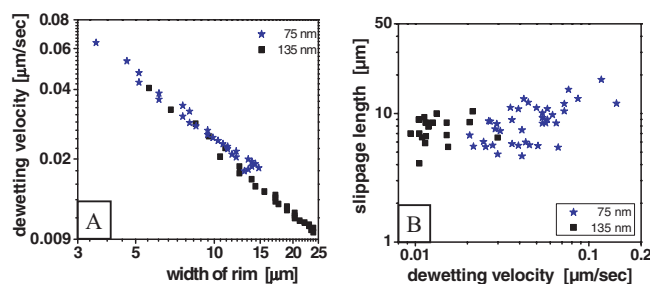


**Fig. 4.** A) Dewetting velocity as a function of the width of the rim and B) slippage length as a function of dewetting velocity on-double logarithmic scales for the system described in Fig. 2 (thicknesses are indicated in the figure).

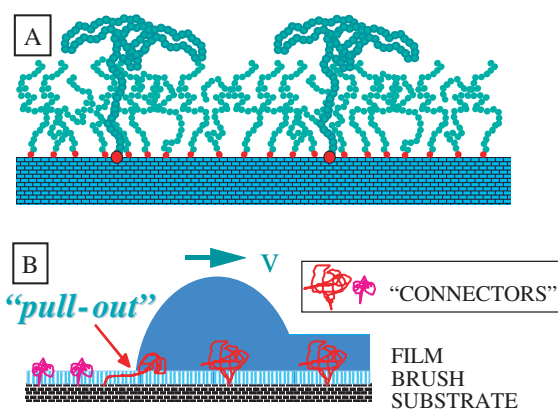


**Fig. 5.** A) Schematic representation of a bimodal polymer brush and B) the corresponding “pull-out” process in the course of dewetting.

The total resisting pull-out force is proportional to number ( $\nu$ ) of connectors times the distance ( $L$ ) the connectors are stretched during the pull-out process (all connectors within  $L$  experience a force):

$$F_p \propto \nu \cdot L \cdot f^*. \quad (4)$$

$f^*$  is the pull-out force per chain which results from two effects [29]. The chains do not want to be exposed to air and as they resist being pulled out, they get stretched, which reduces their entropy.

According to eqs. (3) and (4), dewetting will stop when a certain density of connectors  $\nu_{crit}$  is reached, i.e.  $F_d = F_p$ . This allows to determine  $f^* = F_d/(\nu \cdot L)$ . As the connectors are supposedly fully stretched just before they are pulled out [29], we may write (neglecting the small part embedded in the brush):  $L = N \cdot a$  with  $N$  being the number of monomers of a connector chain and  $a$  being the size of a monomer. In a systematic study using polystyrene molecules [30], independent of their length,  $f^* \approx 10^{-13}N$  has been found for pulling a single polymer chain out of its own melt, simply by systematically determining the dewetting velocity as a function of the density of connectors. This example impressively demonstrates the potential of dewetting experiments for the characterisation of polymer interfaces.

Dewetting also allows to gain insight into the consequences of confining long chain-like polymers into ultra-thin films, sometimes with thicknesses even smaller than the unperturbed size of these macromolecules [18,31–34]. In this context, the influence of film thickness on the value of the glass transition temperature ( $T_g$ ) has drawn a lot of attention [18,32–34]. In our dewetting experiments, we have focused on the influence of sample preparation on the relaxation dynamics for entangled polymer melts [12, 13, 15, 21, 23, 24]. In spite of the complexity of the physical processes at work, dewetting of viscoelastic fluids can be considered as a true rheological probe that offers an outstanding prospect to study polymer dynamics.

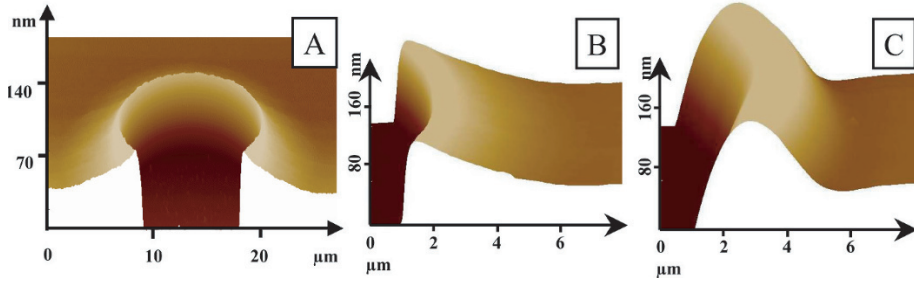


**Fig. 6.** A) 3D-view (measured by atomic force microscopy) of a typical hole obtained by dewetting a polystyrene film on a PDMS-coated substrate at temperatures close to the glass transition of PS. Typical 3D-cross-section of B) the asymmetric shape of the rim at early stages and comparatively low temperatures and C) the more symmetric shape at late stages or at high temperatures.

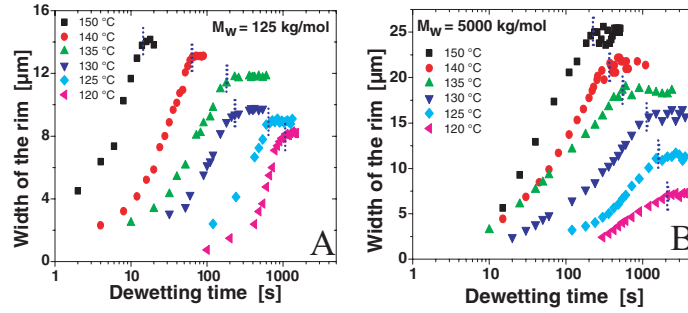


**Fig. 7.** Temporal evolution of the width  $w$  of the rim of holes growing in thin polystyrene films of A)  $M_w = 125$  kD and B)  $M_w = 5000$  kD at various temperatures as indicated in the figures. The times  $\tau$  when  $w$  reached a maximum value are indicated by short dotted lines.

A characteristic feature of dewetting of high molecular weight viscoelastic fluids at temperatures close to  $T_g$  is an asymmetric shape of the rim for long times [12, 13, 15, 21, 23, 24]. Typical examples for the evolution of the shape of the rim are given in Fig. 6. This asymmetric shape results from elastic deformation of the film close to the contact line over a distance which is controlled by interfacial friction. Initially, for small hole diameters, dissipation of the invested energy originating from capillary forces is mainly located within the volume of the film, the removed material (proportional to the dewetted distance  $d$ ) will be redistributed within the film over a certain distance  $\Delta_0$  which is characterized by film thickness  $h$  and frictional properties [7, 19, 21]:

$$d \ll \Delta_0 \sim (h\eta/\zeta)^{1/2} \quad (5)$$

with  $\zeta$  being the friction coefficient at the interface and  $\eta$  the viscosity of the film. In such a situation, there will be no rim formed next to the dewetted zone.

However, with increasing hole diameter dissipation at the film-substrate interface becomes dominant and a rim with a highly asymmetric shape will start to appear. It has a steep side reaching a height ( $H$ ) next to the three-phase contact line and an exponential decay on the other side, with a decay length  $\Delta_0$ .

As in dewetting experiments with simple (Newtonian) fluids, one can also measure the width  $w$  of the rim. The exponential decay is truncated when the height of the rim (measured from the substrate level) has decayed to a value about  $1.1h$ . Then, according to theory [19, 21],  $w = \sqrt{2} \cdot \Delta_0 \cdot \ln(10t/\tau)$ , with  $\tau$  being a characteristic relaxation time of the polymer. As can be seen in Fig. 7 for dewetting experiments performed at different temperatures and for two differently long polymers,  $w$  increased approximately logarithmically in time until it reached a maximum value. Interestingly, for the longer polymer, the time  $\tau_w$  when this maximum is reached was drastically shorter than the longest relaxation time of the polymer in an equilibrated bulk, the reptation time  $\tau_{rep}$ . In Fig. 8, we present a comparison of the values of  $\tau_w$  for the two studied

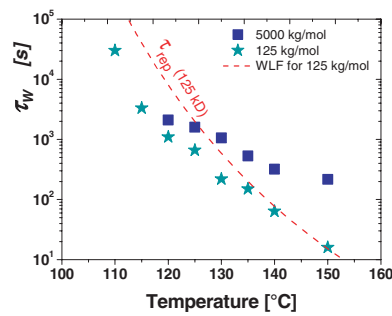


Fig. 8. Evolution of  $\tau$  with temperatures for the measurements shown in Fig. 7.

chain lengths. While the shorter chains approximately followed a WLF behavior [35,36], and at high temperatures the values of  $\tau_w$  and  $\tau_{rep}$  were almost identical, the longer polymer showed significant deviations from such behavior. At the lowest temperatures, we did not observe any influence of molecular weight. The values of  $\tau_w$  were identical for the two polymers studied and  $\tau_w$  seemed to decrease according to a WLF dependence. At higher temperatures, however,  $\tau_w$  varied only slightly with temperature, much less than expected from a WLF behavior. In addition, for the longer polymer, all values of  $\tau_w$  were several orders of magnitude lower than  $\tau_{rep}$  in bulk.

We tentatively interpret  $\tau_w$  as the time needed to relax residual stresses within the spin-coated polystyrene films where chains are trapped in strongly out-of-equilibrium conformations. These conformations have been generated by rapid solvent evaporation in the course of film preparation [37–40]. We anticipate that the entanglement density in the dry spincoated film is lower than in an equilibrated bulk system. As an ultimate limit, PS films can be composed of an assembly of almost independent, non-entangled, fully collapsed polymers.

## 4 Conclusions

In summary, besides their exceptional potential for an insightful characterization of rheological properties of polymer thin films (e.g., the stress relaxation time  $\tau_w$ ), dewetting experiments have been shown to represent also a highly sensitive tool for determining contact angle and frictional properties of polymer/substrate interfaces. In combination with theoretical predictions, we can explore the slippage length at polymer-polymer interfaces and the influence of energy dissipation mechanisms on the dewetting process. Furthermore, using model systems, we can even determine molecular forces necessary for extracting a polymer from its own melt. Systematic dewetting experiments provide a means for determining characteristic relaxation processes in thin polymer films as a function of temperature and molecular weight. Our preliminary results indicate significant deviations from bulk properties. Systematic studies on variously coated substrates allow to exploit the full potential of dewetting for studies of interfacial properties like friction and adhesion at polymer-polymer interfaces.

Both teams from France acknowledge partial financial support from the European Community's "Marie-Curie Actions" under contract MRTN-CT-2004-504052 [POLYFILM]. P. Damman is a Research Associate of the FNRS.

## References

1. P.-G. de Gennes, F. Brochard-Wyart, D. Quéré, *Capillarity and Wetting Phenomena: Drops, Bubbles, Pearls, Waves* (Springer, Heidelberg, 2003)
2. C. Redon, F. Brochard-Wyart, F. Rondelez, Phys. Rev. Lett. **66**, 715 (1991)
3. G. Reiter, Phys. Rev. Lett. **68**, 75 (1992)

4. F. Brochard-Wyart, C. Redon, *Langmuir* **8**, 2324 (1992)
5. F. Brochard-Wyart, P. Martin, C. Redon, *Langmuir* **9**, 3682 (1993)
6. C. Redon, J.B. Brzoka, F. Brochard-Wyart, *Macromolecules* **27**, 468 (1994)
7. F. Brochard-Wyart, G. Debrégeas, R. Fondécave, P. Martin, *Macromolecules* **30**, 1211 (1997)
8. G. Debrégeas, P.-G. de Gennes, F. Brochard-Wyart, *Science* **279**, 1704 (1998)
9. G. Reiter, R. Khanna, *Phys. Rev. Lett.* **85**, 2753 (2000)
10. G. Reiter, R. Khanna, *Langmuir* **16**, 6351 (2000)
11. R. Seemann, S. Herminghaus, K. Jacobs, *Phys. Rev. Lett.* **87**, 196101 (2001)
12. G. Reiter, *Phys. Rev. Lett.* **87**, 186101 (2001)
13. P. Damman, N. Baudelet, G. Reiter, *Phys. Rev. Lett.* **91**, 216101 (2003)
14. J.H. Xavier, Y. Pu, C. Li, M.H. Rafailovich, J. Sokolov, *Macromolecules* **37**, 1470 (2004)
15. G. Reiter, M. Hamieh, P. Damman, S. Slavovs, S. Gabriele, T. Vilmin, E. Raphaël, *Nat. Mater.* **4**, 754 (2005)
16. R. Seemann, S. Herminghaus, C. Neto, S. Schlagowski, D. Podzimek, R. Konrad, H. Mantz, K. Jacobs, *J. Phys.: Condens. Matter* **17**, S267 (2005)
17. M. Rauscher, A. Münch, B. Wagner, R. Blossey, *Eur. Phys. J. E* **17**, 373 (2005)
18. C.B. Roth, B. Deh, B.G. Nickel, J.R. Dutcher, *Phys. Rev. E* **72**, 021802 (2005)
19. T. Vilmin, E. Raphaël, *Europhys. Lett.* **72**, 781 (2005); *Eur. Phys. J. E* **21**, 161 (2006)
20. M.H. Yang, S.Y. Hou, Y.L. Chang, A.C.-M. Yang, *Phys. Rev. Lett.* **96**, 066105 (2006)
21. T. Vilmin, E. Raphaël, P. Damman, S. Slavovs, S. Gabriele, M. Hamieh, G. Reiter, *Europhys. Lett.* **73**, 906 (2006)
22. R. Fetzer, M. Rauscher, A. Mnch, B.A. Wagner, K. Jacobs, *Europhys. Lett.* **75**, 638 (2006)
23. S. Gabriele, P. Damman, S. Scalvons, S. Desprez, S. Coppée, G. Reiter, M. Hamieh, S. Al Akhrass, T. Vilmin, E. Raphaël, *J. Polym. Sci. B Polym. Phys.* **44**, 3022 (2006)
24. P. Damman, S. Gabriele, S. Coppée, S. Desprez, D. Villiers, T. Vilmin, E. Raphaël, M. Hamieh, S. Al Akhrass, G. Reiter, *Phys. Rev. Lett.* **99**, 036101 (2007)
25. A. Casoli, M. Brendlé, J. Schultz, P. Auroy, G. Reiter, *Langmuir* **17**, 388 (2001)
26. L. Bureau, L. Léger, *Langmuir* **20**, 4523 (2004)
27. P.-G. de Gennes, *C.R. Acad. Sci. B* **288**, 219 (1979)
28. H.R. Brown, *Science* **263**, 1411 (1994)
29. E. Raphaël, P.-G. de Gennes, *J. Phys. Chem.* **96**, 4002 (1992)
30. G. Reiter, J. Schultz, P. Auroy, L. Auvray, *Europhys. Lett.* **33**, 29 (1996)
31. G. Reiter, *Europhys. Lett.* **23**, 579 (1993); *Macromolecules* **27**, 3046 (1994)
32. J.A. Forrest, K. Dalnoki-Veress, *Adv. Coll. Interf. Sci.* **94**, 167 (2001)
33. G. Reiter, J. Forrest, *Eur. Phys. J. E* **8**, 101 (2002)
34. P.A. O'Connell, G.B. McKenna, *Science* **307**, 1760 (2005)
35. D.J. Plazek, V.M. O'Rourke, *J. Polym. Sci. A* **9**, 209 (1971)
36. A. Bach, K. Almdal, H.K. Rasmussen, O. Hassager, *Macromolecules* **36**, 5174 (2003)
37. S.G. Croll, *J. Appl. Polym. Sci.* **23**, 847 (1979)
38. B.B. Sauer, D.J. Walsh, *Macromolecules* **27**, 432 (1994)
39. G. Reiter, P.-G. de Gennes, *Eur. Phys. J. E* **6**, 25 (2001)
40. L. Si, M.V. Massa, K. Dalnoki-Veress, H.R. Brown, R.A.L. Jones, *Phys. Rev. Lett.* **94**, 127801 (2005)